Free Radical Research, April 2011; 45(4): 389–399

informa
healthcare

Hydrogen peroxide induces Beclin 1-independent autophagic cell death by suppressing the mTOR pathway via promoting the ubiquitination and degradation of Rheb in GSH-depleted RAW 264.7 cells

GIMOON SEO[1,2], SEONG KEUN KIM[1,2], YU JEONG BYUN[3], EUNHYE OH[1,2], SEONG-WHAN JEONG[3], GUE TAE CHAE[1,2] & SEONG-BEOM LEE[1,2]

[1]*Institute of Hansen's Disease,* [2]*Department of Pathology, and* [3]*Department of Biochemistry, College of Medicine, The Catholic University of Korea, 505 Banpo-dong, Seocho-gu, Seoul 137-701, Korea*

(Received date: 6 September 2010; Accepted date: 17 October 2010)

Abstract

A novel mechanism for H_2O_2-induced autophagic cell death in GSH-depleted RAW 264.7 cells, a murine macrophage cell line, is proposed. Under GSH-depleted conditions, H_2O_2-induced autophagic cell, characterized by an increased LC3-II/I ratio, a decreased level of p62 and the formation of autophagic vacuoles, was inhibited by bafilomycin A1 and by *Atg5* siRNA transfection, whereas the cell death was not inhibited by zVAD-fmk, by PI3K inhibitors or by *Beclin 1* siRNA transfection. In addition, H_2O_2 treatment reduced the activity of mTOR and promoted the ubiquitination and degradation of Rheb, a key upstream activator of mTOR. Furthermore, proteasome inhibition with MG132 restored the expression of Rheb and increased mTOR activity, resulting in an increased viability of H_2O_2-treated cells. Collectively, these findings demonstrate that H_2O_2 induces Beclin 1-independent autophagic cell death by suppressing the mTOR pathway via promoting the ubiquitination and degradation of Rheb in GSH-depleted RAW 264.7 cells.

Keywords: *Hydrogen peroxide, autophagic cell death, mTOR, Rheb, ubiquitination, glutathione*

Abbreviations: *H_2O_2, hydrogen peroxide; GSH, glutathione; LC3, microtubule-associated light chain3; PI3K, phosphatidylinositol 3-kinase; mTOR, mammalian target of rapamycin; p70S6K, p70 ribosomal protein S6 kinase; Rheb, Ras homologue enriched in brain; BNIP3, Bcl-2/E1B 19 kDa interacting protein 3; UPS, ubiquitin-proteasome system; 3-MA, 3-Methyladenine; BSO, L-Buthionine sulphoximine; DMSO, dimethyl sulphoximide; MPP+, 1-methyl-4-phenylpyridinium; ERK, extracellular signal-regulated protein kinase; MTT, 3-(4,5-dimethylthiazol-2-yl)-2,5-diphenyl-tetrazolium bromide; MG132, Carbobenzoxy-Leu-Leu-leucinal; Atg, autophagy-related gene; Bcl-2, B-cell lymphoma protein-2.*

Introduction

H_2O_2 is converted to hydroxyl radicals through the Fenton reaction and causes oxidative damage to DNA, membrane lipids and cellular proteins [1]. To protect against H_2O_2 damage, mammalian cells maintain H_2O_2 levels by removing H_2O_2 through antioxidant systems such as catalase, peroxiredoxin and glutathione peroxidase [2]. Despite these antioxidant systems, H_2O_2 induces either necrosis or apoptosis depending on its concentration and the specific cell type [3,4]. In addition, H_2O_2 has also been reported to induce autophagy and/or autophagic cell death in certain circumstances [5].

While the details of the mechanism of H_2O_2-induced autophagy are unclear, several mechanisms for the effect of H_2O_2 on autophagy in various cells have been proposed. One is that increased H_2O_2, as the result of nutrient starvation, inactivates Atg4, a cysteine protease, which cleaves Atg8, or microtubule-associated light chain (LC)-3, thereby enhancing Atg8 lipidation and autophagosome formation in CHO cells [6]. The formation of lipidated Atg8 is an essential component in the process of autophagosome formation. The other

Correspondence: Dr Seong-Beom Lee, Institute of Hansen's Disease, Department of Pathology, College of Medicine, The Catholic University of Korea, 505 Banpo-dong, Seocho-gu, Seoul, South Korea. Tel: +82 2 2258 7313. Fax: +82 2 595 2241. Email: sblee@catholic.ac.kr

ISSN 1071-5762 print/ISSN 1029-2470 online
DOI: 10.3109/10715762.2010.535530

mechanism proposes that the formation of a complex between Beclin 1 and a class III phosphatidylinositol 3-kinase (PI3K) is an essential step in the initiation of autophagy in various H_2O_2-treated cells, including HEK293, U87, HeLa and U251 cells [5,7]. Another proposal is that increased levels of Bcl-2/E1B 19 kDa interacting protein 3 (BNIP3) produced by H_2O_2 induces autophagic cell death in glutathione (GSH)-depleted C6 cells [8]. BNIP3 induces autophagic cell death in various ways, i.e. by binding to and inhibiting Bcl-2, an inhibitor of Beclin 1 [9], by directly damaging mitochondria [10] and by inhibiting the mammalian target of rapamycin (mTOR)/p70 ribosomal protein S6 kinase (p70S6K) pathway through binding to Ras homologue enriched in brain (Rheb), a key upstream activator of mTOR [11]. Rheb is involved in the regulation of protein translation and autophagy by controlling mTOR activity [12].

In addition to autophagy, H_2O_2 has been reported to stimulate the ubiquitin-proteasome system (UPS) [13]. The UPS, in which proteins are selectively targeted for degradation by covalent ligation to ubiquitin, plays an important role in various cellular processes, including the cell cycle, signal transduction, receptor-mediated endocytosis, antigen presentation, the quality control of proteins and apoptosis [14,15]. The UPS has also been implicated in the regulation of autophagy [16]. Proteasome inhibition has been shown to induce autophagy, suggesting that autophagy functions as a compensatory mechanism in response to accumulated UPS substrates [17]. However, little is known about how the UPS regulates autophagic cell death in the context of oxidative stress.

We report herein on an investigation of the mechanism underlying the H_2O_2-induced cell death in GSH-depleted RAW 264.7 cells, a murine macrophage cell line. GSH, especially mitochondrial GSH, is essential in protecting cellular organelles from damage by H_2O_2. It is removed by glutathione peroxidase, which requires GSH as an electron donor. Thus, any depletion of GSH would be expected to result in an increase in H_2O_2 levels [18,19] and to aggravate the cytotoxic effect of H_2O_2. A number of previous studies on the effects of reactive oxygen species (ROS), including H_2O_2, under GSH-depleted conditions have been reported [8,20]. In the present study, we also depleted cellular GSH by treatment with BSO (L-Buthionine sulphoximine), a GSH synthesis inhibitor, in an attempt to clarify the effects of H_2O_2.

We initially attempted to characterize the cytotoxic effect of H_2O_2 on GSH-depleted RAW 264.7 cells. H_2O_2 treatment induced autophagic cell death, characterized by an increased LC3-II/I ratio, a decreased level of p62 and the formation of autophagic vacuoles. H_2O_2-induced cell death was inhibited by bafilomycin A1 and by *Atg5* siRNA transfection, whereas the cell death was not inhibited by zVAD-fmk, by PI3K inhibitors or *Beclin 1* siRNA transfection. In addition, H_2O_2 reduced mTOR activity and promoted the ubiquitination and degradation of Rheb. Furthermore, proteasome inhibition with MG132 (Carbobenzoxy-Leu-Leu-leucinal) restored the expression of Rheb and increased mTOR activity, resulting in an increased viability of H_2O_2-treated cells. Our results demonstrate that, under GSH-depleted conditions, H_2O_2 induces Beclin 1- independent autophagic cell death by suppressing the mTOR pathway via promoting the ubiquitination and degradation of Rheb in RAW 264.7 cells.

Materials and methods

Reagents and antibodies

H_2O_2, Staurosporine, BSO, cycloheximide, bafilomycin A1, 3-Methyladenine (MA), wortmannin and trypan blue were obtained from Sigma Aldrich Co. Ltd (St. Louis, MO). zVAD-fmk was obtained from Tocris Bioscience (Ellisville, MO). MG132 was obtained from Calbiochem (La Jolla, CA). MTT [3-(4,5-dimethylthiazol-2-yl)-2,5-diphenyl-tetrazolium bromide] was obtained from Duchefa Biochemie (Haarlem, Netherlands). Bafilomycin A1, zVAD-fmk and MG132 were dissolved in DMSO. The final vehicle concentration was adjusted to 0.1% (v/v) and the control medium contained the same quantity of vehicle. Antibodies against p62, Beclin 1, BNIP3, Atg5, p-p70S6K, p70S6K, p-mTOR, mTOR, Rheb and LC3 were obtained from Cell Signaling Technology (Beverly, MA). Antibodies against GAPDH and horseradish peroxidase were obtained from Santa Cruz Biotechnology (Santa Cruz, CA). Antibody against ubiquitin was obtained from Abcam PLC (Cambridge, UK).

Cell culture

RAW 264.7 cells, a murine macrophage cell line, were acquired from ATCC (Manassas, VA) and were maintained in Dulbecco's Modified Eagle's medium (GIBCO BRL, Grand Island, NY) containing 20 mM HEPES (Fisher scientific, Atlanta, GA), 10% FBS (GIBCO BRL), 100 U/ml of penicillin and 100 μg/ml of streptomycin (Bio Whittaker Inc., Walkersville, MD) at 37°C in 5% CO_2. The cells were plated onto 6- or 96-well plates.

Inhibitor treatments

Cells were plated onto 6- or 96-well plates with 50 μM BSO, a GSH synthesis inhibitor. After 24 h, the cells were pre-treated with the designated inhibitors for 1 or 2 h and followed by treatment with H_2O_2 at the indicated concentrations for 2 h. After incubation for the designated time, the cells were harvested for the next experiment. The inhibitors were used at the following concentrations: zVAD-fmk, 20 μM; 3-MA,

5 mM; wortmannin, 200 nM; Bafilomycin A1, 50 nM; MG132, 20 μM; and cycloheximide, 20 μM. The concentrations of inhibitors used in these studies were chosen based on the results of previous studies [8,21–25].

GSH assay

Cells were plated with various concentrations of BSO. After 24 h, the intracellular level of total GSH was determined by a GSH assay kit (Cayman Chemical, Ann Arbor, MI) according to the manufacturer's protocol, as described previously [26].

Cell viability assay

Cell viability was measured by an MTT reduction assay or a trypan blue exclusion assay in 96-well plates as described previously [18,27].

Western blot analysis

The treated cells were removed from the incubator at designated times and placed on ice. The cells were then washed three times with ice-cold PBS. They were then lysed for 30 min with RIPA lysis buffer (50 mM Tris-HCl (pH 7.4), 1% Triton X-100, 150 mM NaCl, 0.1% SDS, 0.5% sodium deoxycholate, 100 mM phenylmethylsulphonyl fluoride, 1 μg/ml of leupeptin, 1 mM Na_3VO_4 and 1× Complete™ Protease Inhibitor Cocktail (Santa Cruz Biotechnology)). Equal amounts of protein were loaded onto 10–15% SDS-PAGE gels, electrophoresed and transferred onto PVDF membranes (Millipore, Bedford, MA). The membranes were blocked by treatment with Tris-Buffered Saline with 0.05% Tween 20 (TBST) supplemented with 5% powdered milk or 5% BSA and then incubated with primary antibodies against the designated proteins. The blots were then washed with TBST and incubated with a horseradish peroxidase-conjugated secondary antibody in TBST plus 5% powdered milk. The bound antibodies were detected with Super Signal Ultra chemiluminescence reagents (Pierce Biotechnology, Inc., Rockford, IL).

Electron microscopy

Cells were fixed with 2.5% glutaraldehyde for 2 h, post-fixed by treatment with 1% osmium tetroxide, dehydrated in ethanol and embedded in Epon 812 (Polyscience, Warrington, PA). Ultra-thin sections were contrasted with uranyl acetate and lead citrate. Sections were examined by transmission electron microscopy (JEOL, Arishima, Japan).

Beclin 1,BNIP3, Rheb and Atg5 siRNA transfections

For silencing Beclin 1, BNIP3, Rheb and Atg5 genes, *Beclin 1*-directed siRNA pool (ON-TARGET *plus SMART*pool reagent L-055895-00-0005), *BNIP3*-directed siRNA pool (ON-TARGET *plus SMART*pool reagent L-040256-01-0005) and *Rheb*-directed siRNA pool (ON-TARGET *plus SMART*-pool reagent L-057044-00-0005) were purchased from Dharmacon (Lafayette, CO). *Atg5*-directed siRNA was purchased from Ambion (Austin, TX). The sequence of *Atg5* siRNA is 5'-ACC GGA AAC TCA TGG AAT A-3'. Negative control siRNA was purchased from Dharmacon. Cells were transfected with *Beclin 1*, *BNIP3*, *Rheb*, *Atg5* or control siRNA by electroporation under conditions of 1350 voltage and 35 ms using a pipette-type electroporator (MicroPorator-Mini, Digital Bio Technology, Suwon, Kyounggi-do, Korea) according to the manufacturer's instructions. The efficiency of the siRNA silencing of the designated gene was confirmed by western blot analysis at 48 h after transfection.

Reverse transcriptase (RT)-PCR

The expression of *Rheb* mRNA was determined by RT-PCR. In this procedure, total RNA was extracted using a High Pure RNA isolation kit (Roche Diagnostics, Mannheim, Germany) and converted to cDNA using an Advantage RT-for-PCR kit (Clontech, Hampshire, UK), according to the manufacturer's instructions. To confirm *Rheb* mRNA expression, PCR was performed at 94°C for 3 min followed by 35 cycles of amplification (94°C for 1 min, 58.5°C for 1 min, and 72°C for 30 s). The following primers for *Rheb* and *GAPDH* were used: For *Rheb*, forward primer (5'-CTG CCC GTC ATC CTT GAA-3') and reverse primer (5'-GAC GTT AAC ATA ATC TGA AAG-3'). For *GAPDH*, forward primer (5'-GGG AAG CTC ACT GGC ATG G-3') and reverse primer (5'-CTT CTT GAT GTC ATC ATA CTT GGC AG-3'). The PCR products were then separated on a 2% polyacrylamide gel.

Rheb ubiquitination assay

Rheb ubiquitination was assessed using an ubiquitin enrichment kit (Pierce, Rockford, IL) and western blot analysis. Ubiquitin-enriched cell lysates were obtained according to the manufacturer's protocol. Briefly, the treated cells were lysed with RIPA buffer and the protein content of the lysate was adjusted so as to contain 300 μg per sample. The lysate was then incubated with a polyubiquitin affinity resin in a spin column at 4°C for 24 h on an end-over-end rotator. The column was washed with washing buffer (one part RIPA buffer with nine parts TBS) and the ubiquitin-enriched fraction was then eluted with SDS-PAGE loading buffer. The eluted samples were analysed by western blot analysis with an anti-Rheb antibody.

Statistical analysis

All results are expressed as the mean ± SEM. The interactions of the main effects of BSO pre-treatment

and the different siRNAs were statistically analysed by two-way analysis of variance (ANOVA). The statistical significance of the difference from the respective controls for each experimental condition was determined by means of an unpaired Student's *t*-test. $p < 0.01$ was considered to be statistically significant.

Results

H_2O_2 induces autophagic cell death in GSH-depleted RAW 264.7 cells

We initially assessed the cytotoxic effects of H_2O_2 on RAW 264.7 cells via an MTT reduction assay. As shown in Figure 1A, treatment with H_2O_2 for 2 h in the presence of BSO reduced the levels of cell viability in a dose-dependent manner. In this study, to examine the cytotoxic effect of H_2O_2, we pre-treated cells with 50 μM BSO for 24 h, prior to H_2O_2 treatment. Treatment with H_2O_2 for 2 h in the presence of 50 μM BSO, a dosage capable of completely abolishing GSH levels (Figure 2A), significantly reduced cell viability compared to cells treated in the absence of BSO (Figure 1A, $p < 0.001$). However, BSO itself at 50 μM did not show cytotoxicity in RAW 264.7 cells for periods of up to 24 h (Figure 2B).

To characterize the cytotoxic effects of H_2O_2 on GSH-depleted RAW 264.7 cells, we next examined the issue of whether H_2O_2-induced cell death is dependent on the autophagic or apoptotic pathway. Pre-treatment with 50 nM bafilomycin A1, a specific inhibitor of vacuolar type H+-ATPase, resulted in a significant increase in cell viability compared to control cells treated with the same concentration of H_2O_2 in GSH-depleted RAW 264.7 cells (Figure 1B, $p < 0.001$). Bafilomycin A1 has been reported to inhibit autophagy at a later stage by inhibiting fusion between autophagosomes and lysosomes [28]. However, pre-treatment with 20 μM zVAD-fmk, a pan-caspase inhibitor, had no effect on the viability of H_2O_2-treated and GSH-depleted RAW 264.7 cells (Figure 1B). In addition, we measured the level of p62 expression and the ratio of LC3-II to LC3-I in H_2O_2-treated and GSH-depleted RAW 264.7 cells at 2 h after H_2O_2 treatment. p62 is incorporated into autophagosome and is degraded in autolysosomes. LC3, a mammalian homologue of yeast Atg8, is conjugated to the autophagosomal membrane. For this, LC3 undergoes a shift from

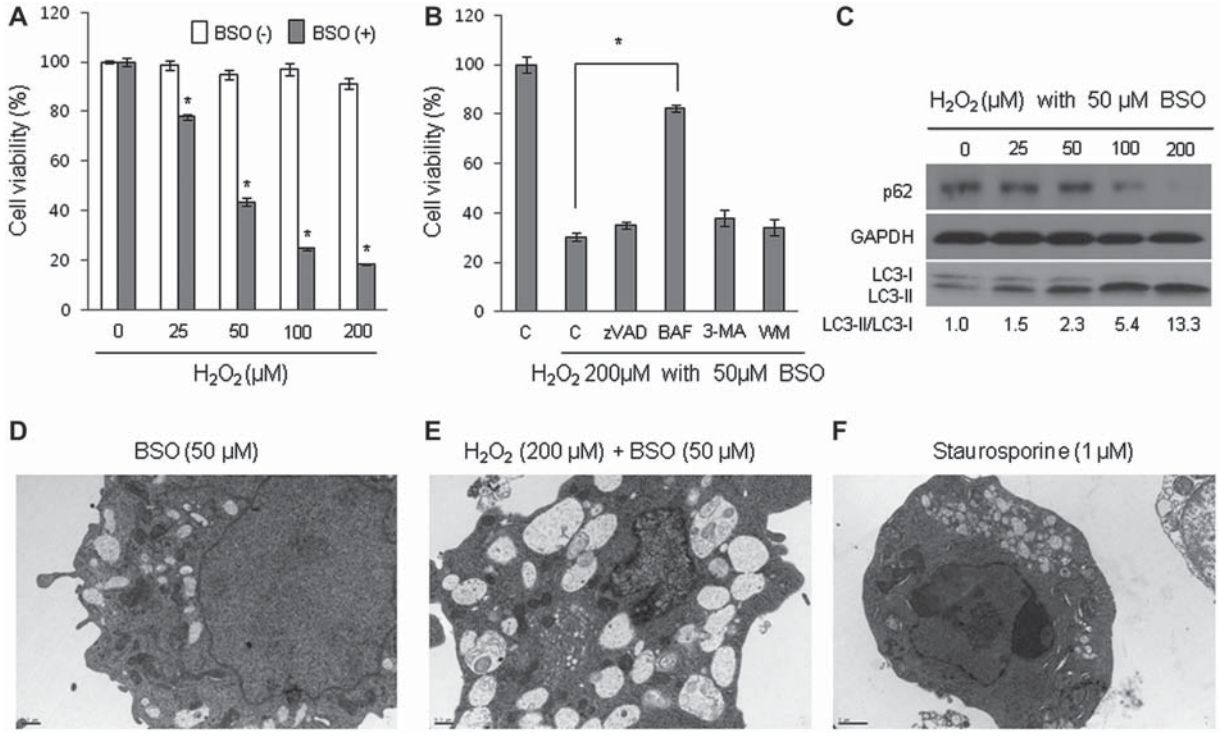

Figure 1. H_2O_2 induces autophagic cell death in GSH-depleted RAW 264.7 cells. (A and C) The cells were pre-treated or not with 50 μM BSO, a GSH synthesis inhibitor, for 24 h, followed by treatment with H_2O_2 at the indicated concentrations for 2 h. (A) Cell viability was assessed by an MTT reduction assay at 2 h after H_2O_2 treatment. (B) Cells were pre-treated with 50 μM BSO for 24 h and then treated with zVAD-fmk (zVAD, 20 μM), bafilomycin A1 (BAF, 50 nM), 3-MA (5 mM), wortmannin (WM, 200 nM) or DMSO for 1 h before the addition of 200 μM H_2O_2. Cell viability was assessed by an MTT reduction assay at 2 h after H_2O_2 treatment. (C) The expression level of p62 and the LC3-II/I ratio were determined by western blot analysis at 2 h after H_2O_2 treatment. (D–F) The ultrastructural morphology of the cells was examined by transmission electron microscopy. For electron microscopic analysis, the cells were pre-treated with 50 μM BSO for 24 h, followed by treatment with 200 μM H_2O_2 for 2 h. As a positive control for apoptosis, cells were treated only with 1 μM staurosporine for 24 h (F). Similar results were observed in three independent experiments. $^*p < 0.001$ vs control cells treated with same H_2O_2 concentrations. Scale bars: 0.5 μm (D and E) and 1 μm (F).

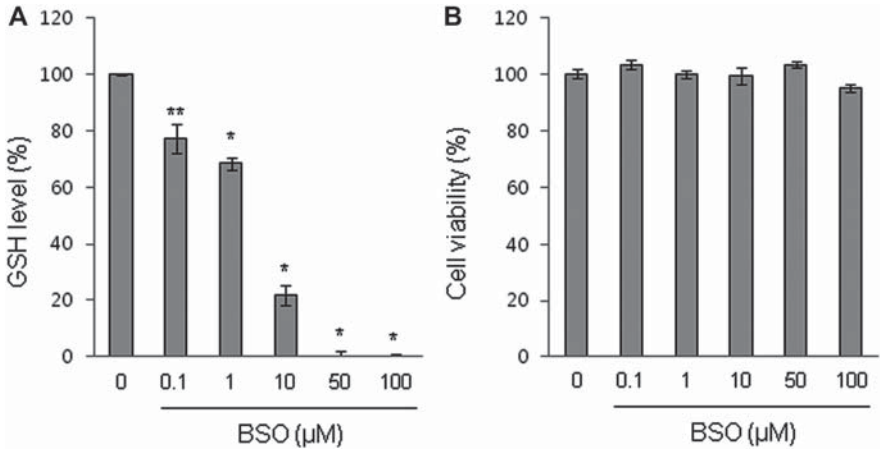

Figure 2. Treatment with BSO reduces the level of GSH in RAW 264.7 cells. The cells were treated or not treated with BSO at the indicated concentrations for 24 h. (A) The intracellular level of GSH was determined by a GSH assay kit. (B) Cell viability was assessed by an MTT reduction assay. $^{*}p < 0.001$ and $^{**}p < 0.01$ vs BSO non-treated control cells.

the cytosolic form (LC3-I) to the membrane-bound form (LC3-II). Thus, the level of the p62 protein and the LC3-II/I ratio serve as indicators of the extent of autophagosome formation [29]. As shown in Figure 1C, treatment with H_2O_2 resulted in a significant down-regulation in the levels of p62 expression and an increase in the LC3-II/I ratios in a dose-dependent manner, compared to that for the control treatment under GSH-depleted conditions. We also examined the ultrastructural morphology of H_2O_2-treated and GSH-depleted cells. Cells treated with 200 μM H_2O_2 for 2 h contained numerous autophagic vacuoles that contained cytoplasmic materials (Figure 1E), but not the characteristic features of apoptosis, whereas cells treated with 1 μM staurosporine for 24 h showed both autophagic vacuoles and apoptotic findings such as chromatin condensation (Figure 1F) compared to control cells (Figure 1D). Collectively, the results reported herein demonstrate that H_2O_2 induces caspase-independent autophagic cell death in GSH-depleted RAW 264.7 cells.

H_2O_2-induced autophagic cell death is not dependent on Beclin 1/class III PI3K and BNIP3 in GSH-depleted RAW 264.7 cells

Beclin 1 forms a complex with class III PI3K and the complex is required for autophagy under conditions of nutrient starvation [30]. Thus, we examined the role of Beclin 1 and class III PI3K in H_2O_2 -induced autophagic cell death in GSH-depleted RAW 264.7 cells. However, treatment with H_2O_2 for 2 h did not stimulate an increase in Beclin 1 expression (Figure 3A) and the down-regulation of *Beclin 1* by siRNA transfection (Figure 3B) had no effect on the viability of H_2O_2-treated cells compared to cells transfected with control siRNA (Figure 3C) under GSH-depleted conditions. In addition, its viability was not recovered by treatment with PI3K inhibitors, such as 3-MA and wortmannin (Figure 1B).

We previously reported that, in GSH-depleted C6 glioma cells, H_2O_2-induced autophagic cell death is dependent on BNIP3 [8]. Thus, we assessed whether BNIP3 is involved in H_2O_2-induced autophagic cell death in RAW 264.7 cells. However, in GSH-depleted RAW 264.7 cells, the down-regulation of *BNIP3* by siRNA transfection (Figure 3B) did not rescue cells from H_2O_2-induced cell death compared to cells transfected with control siRNA (Figure 3D), although treatment with H_2O_2 for 2 h resulted in a significant increase in BNIP3 expression compared to that for a control treatment under GSH-depleted conditions (Figure 3A). However, the down-regulation of *Atg5* by siRNA transfection (Figure 3B) protected cells from H_2O_2-induced cell death compared to cells that had been transfected with control siRNA (Figure 3E), suggesting that autophagy induced by H_2O_2 functions as a cell death rather than a protective mechanism in GSH-depleted RAW 264.7 cells. With other Atg proteins, Atg5 plays an important role in the formation of autophagosome [31]. These results demonstrate that H_2O_2 -induced autophagic cell death, in GSH-depleted RAW 264.7 cells, is not dependent on Beclin 1/class III PI3K and BNIP3.

H_2O_2 reduces phosphorylation of mTOR at Ser 2481 and p70S6K at Thr 389 in GSH-depleted RAW 264.7 cells

We next assessed whether H_2O_2 affected the mTOR pathway, since the suppression of the mTOR pathway has been reported to play an important role in Beclin 1/class III PI3K-dependent as well as -independent autophagy [32]. As shown in Figure 4, under GSH-depleted conditions, treatment with H_2O_2 for 2 h significantly reduced the phosphorylation of mTOR

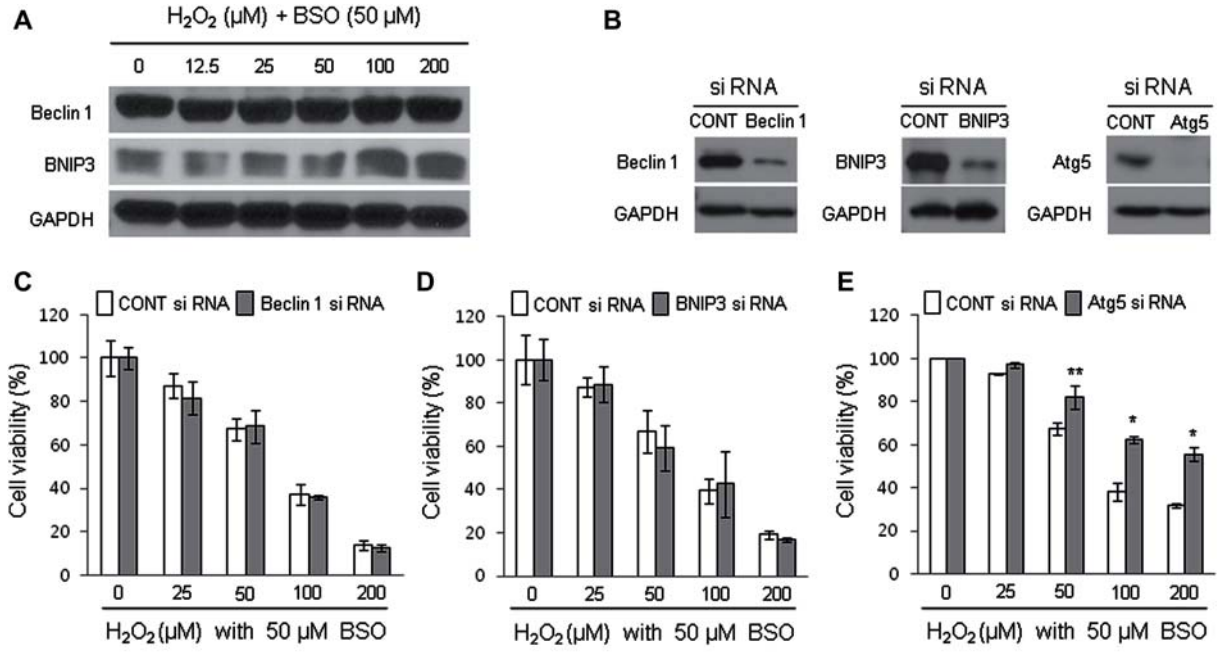

Figure 3. H_2O_2-induced autophagic cell death is not dependent on Beclin 1/class III PI3K and BNIP3 in GSH-depleted RAW 264.7 cells. (A) Cells were pre-treated with 50 μM BSO for 24 h followed by treatment with H_2O_2 at the indicated concentrations for 2 h. The expressions of Beclin 1 and BNIP3 were determined by western blot analysis at 2 h after H_2O_2 treatment. (B–E) Cells were transfected with *Beclin 1* (0.5 μM), *BNIP3* (0.05 μM), *Atg5* (2 μM) or control siRNAs. At 24 h after transfection, the transfected cells were re-plated onto 6- or 96-well plates and pre-treated for 24 h with 50 μM BSO, followed by treatment with H_2O_2 at the indicated concentrations for 2 h. (B) The effects of *Beclin 1*, *BNIP3* and *Atg5* siRNA transfection were confirmed by western blot analysis at 48 h after transfection. (C–E) Cell viability was assessed by an MTT reduction assay at 2 h after H_2O_2 treatment. Similar results were observed in three independent experiments. $^{*}p < 0.001$ and $^{**}p < 0.01$ vs control siRNA-transfected cells treated with same H_2O_2 concentrations.

at Ser 2481 and p70S6K at Thr 389, which were significantly decreased in the presence of 100 and 200 μM H_2O_2. However, the levels of phosphorylation were not correlated with cell viability (Figure 1A) or LC3-II/I ratio (Figure 1C). When treated with 25 or 50 μM H_2O_2, cell viability was reduced (Figure 1A) and LC3-II/I ratio was increased (Figure 1C), whereas the levels of phosphorylation of mTOR at Ser 2481 and p70S6K at Thr 389 were not affected (Figure 4).

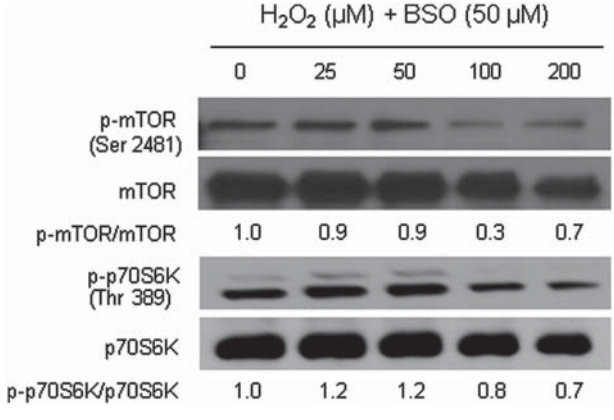

Figure 4. H_2O_2 reduces the phosphorylation of mTOR at Ser 2481 and p70S6K at Thr 389 in GSH-depleted RAW 264.7 cells. Cells were pre-treated with 50 μM BSO for 24 h, followed by treatment with H_2O_2 at the indicated concentrations for 2 h. The degrees of phosphorylation of mTOR at Ser 2481 and p70S6K at Thr 389 were determined by western blot analysis at 2 h after H_2O_2 treatment. Similar results were observed in three independent experiments.

Down-regulation of Rheb by Rheb siRNA induces autophagic cell death in RAW 264.7 cells

We then examined the effect of Rheb down-regulation, a downstream target of BNIP3 and an upstream activator of the mTOR/p70S6K pathway, in RAW 264.7 cells. Rheb, a small GTPase, is negatively regulated by both the tuberous sclerosis complex (TSC) 1/2, a GTPase-activating protein and BNIP3 and it subsequently activates the mTOR complex 1 (mTORC1)/p70S6K pathway [11]. Thus, Rheb has been proposed to play an important role in the regulation of autophagy through the control of the mTOR/p70S6K pathway [33]. As shown in Figure 5, the down-regulation of Rheb by *Rheb* siRNA transfection slightly reduced the extent of phosphorylation of p70S6K at Thr 389, down-regulated the level of p62 expression, increased the LC3-II/I ratio and reduced cell viability in RAW 264.7 cells compared to cells transfected with control siRNA at 48 h after transfection. To rule out the possibility that the slightly reduced MTT level may be due to decreased proliferation in the absence of Rheb rather than reduced cell viability, we measured cell viability using both an MTT and a trypan blue exclusion assay. No significant difference in cell viability was found

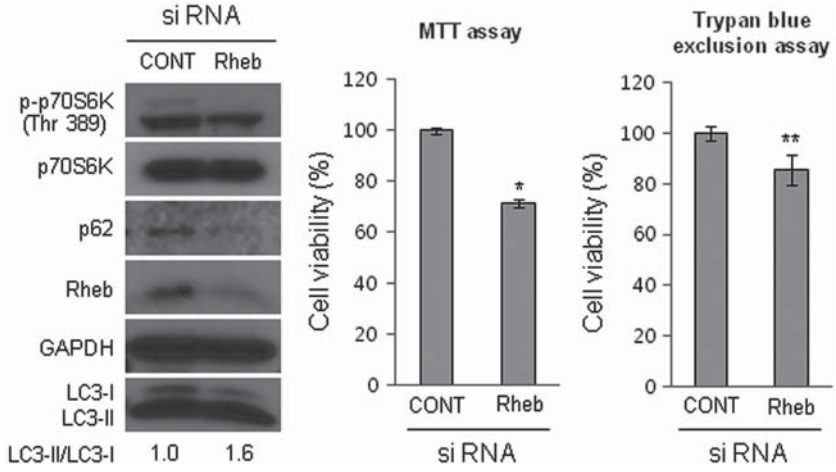

Figure 5. Down-regulation of Rheb by *Rheb* siRNA reduces the phosphorylation of p70S6K at Thr 389, down-regulates p62 expression, increases the ratio of LC3-II/I and reduces cell viability in RAW 264.7 cells. Cells were transfected with *Rheb* and control siRNA. At 24 h after transfection, the transfected cells were re-plated onto 6- or 96-well plates and were used for experiments after further culture for 24 h. (A) The effect of *Rheb* siRNA transfection was confirmed by western blot analysis at 48 h after transfection. The degree of phosphorylation of p70S6K at Thr 389, the level of p62 expression and the LC3-II/I ratio were determined by western blot analysis at 48 h after transfection. (B) Cell viability was assessed by an MTT and a trypan blue exclusion assay at 48 h after transfection. Similar results were observed in three independent experiments. $^{*}p < 0.001$ and $^{**}p < 0.01$ vs control siRNA-transfected cells.

between the two assays (Figure 5B). These results suggest that the down-regulation of Rheb itself is sufficient to induce autophagic cell death via suppression of the mTOR/p70S6K pathway.

H_2O_2 promotes the ubiquitination and degradation of Rheb in GSH-depleted RAW 264.7 cells

We hypothesized that if H_2O_2 decreases Rheb expression, the down-regulation of Rheb by H_2O_2 may play a role in H_2O_2-induced mTOR suppression. Thus, we assessed the role of Rheb down-regulation on mTOR suppression-mediated autophagic cell death in H_2O_2 treated and GSH-depleted cells. As shown in Figure 6, under GSH-depleted conditions, treatment with H_2O_2 for 2 h reduced the expression of Rheb at the protein level, but not at the mRNA level. We then examined

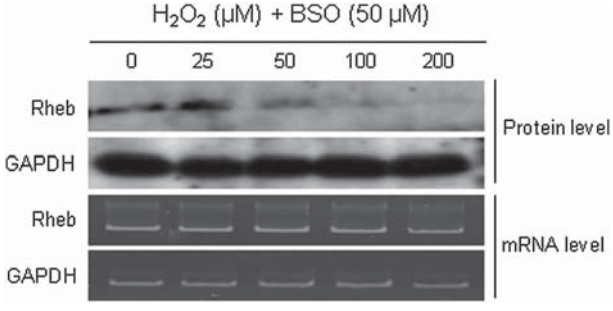

Figure 6. H_2O_2 down-regulates the expression of Rheb at protein level in GHS-depleted RAW 264.7 cells. Cells were pre-treated with 50 μM BSO for 24 h, followed by treatment with H_2O_2 at the indicated concentrations for 2 h. The expression of Rheb was determined at the protein level by western blot analysis and mRNA level by RT-PCR at 2 h after H_2O_2 treatment. Similar results were observed in three independent experiments.

the issue of whether the decreased protein level of Rheb caused by H_2O_2 is due to a reduced stability of the Rheb protein. Treatment with H_2O_2 for 2 h increased the ubiquitination of Rheb under GSH-depleted conditions (Figure 7A). In addition, co-treatment with 20 μM MG132, an ubiquitin-proteasome inhibitor, and 20 μM cycloheximide, an inhibitor of protein synthesis, rescued Rheb protein from H_2O_2-induced degradation and decreased the ratios of LC3-II/I of H_2O_2-treated cells from 30 to 120 min after H_2O_2 treatment, compared with only H_2O_2-treated cells under GSH-depleted conditions (Figure 7B). Furthermore, proteasome inhibition with MG132 restored the expression of Rheb and the levels of phosphorylation of mTOR at Ser 2481 and p70S6K at Thr 389, resulting in an increase in the viability of H_2O_2-treated cells, compared with only H_2O_2-treated cells under GSH-depleted conditions (Figures 8A and B). These results indicate that the degradation of Rheb protein by H_2O_2 involves the ubiquitin-proteasome process and H_2O_2 induces autophagic cell death by suppressing the mTOR/p70S6K pathway via promoting the ubiquitination and degradation of Rheb in GSH-depleted RAW 264.7 cells.

Discussion

In the current study, we provide evidence to show that H_2O_2 promotes the ubiquitination and degradation of Rheb, leading to autophagic cell death in GSH-depleted RAW 264.7 cells via the suppression of mTOR. These results reveal a novel mechanism for H_2O_2-induced autophagic cell death, which is independent of Beclin 1/class III PI3K under GSH-depleted conditions. However, the Beclin 1-independent autophagic cell

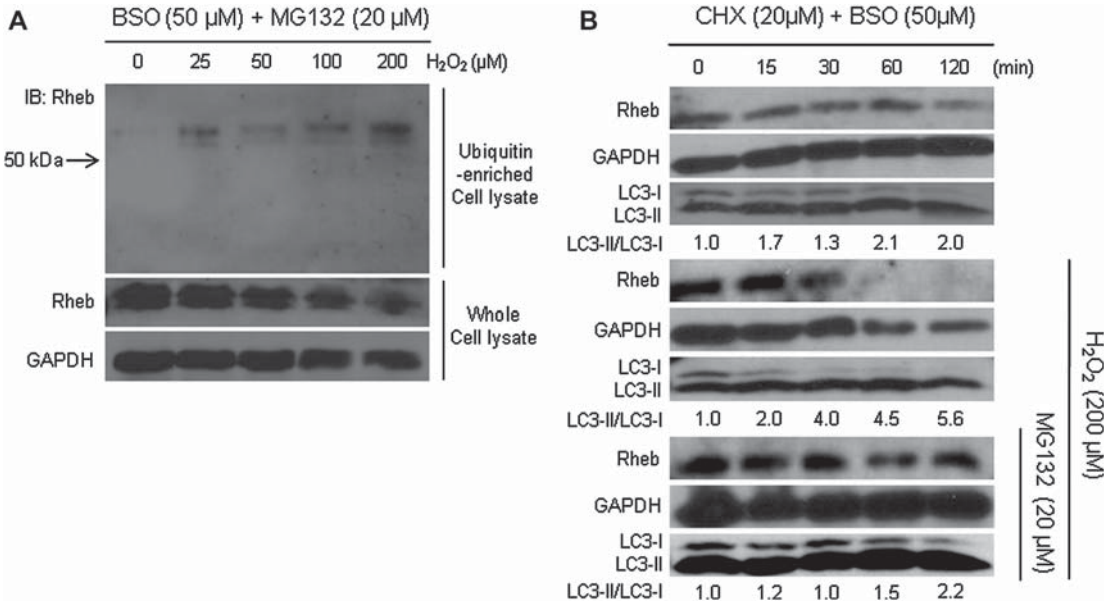

Figure 7. H_2O_2 promotes the ubiquitination and degradation of Rheb in GHS-depleted RAW 264.7 cells. Cells were pre-treated with 50 μM BSO for 24 h and then treated with 20 μM cycloheximide and/or 20 μM MG132 for 2 h, followed by treatment with H_2O_2 at the indicated concentrations for 2 h (A) or with H_2O_2 at 200 μM for the indicated time (B). (A) Ubiquitin-enriched cell lysates were obtained and subjected to western blot analysis using anti-Rheb antibodies. (B) The expression level of Rheb and the LC3-II/I ratio were determined by western blot analysis at the indicated times after H_2O_2 treatment. Similar results were observed in three independent experiments.

death by Rheb degradation in H_2O_2-treated and GSH-depleted RAW 264.7 cells may be cell type or stimulator specific. Thus, further studies will be needed to assess the influence of Rheb degradation on autophagic cell death under various conditions.

GSH is the most abundant thiol antioxidant in mammalian cells. Thus, GSH depletion is generally thought to be necessary for the generation of ROS and to increase the sensitivity of cells to oxidative stress [20]. Our results also showed that GSH-depletion by treatment with 50 μM BSO, a specific inhibitor of GSH synthesis, rendered cells more sensitive to H_2O_2

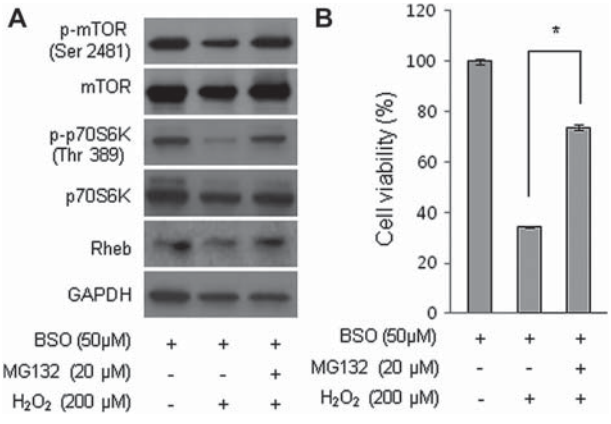

Figure 8. Proteasome inhibition with MG132 protects RAW 264.7 cells from H_2O_2-induced autophagic cell death under GSH-depleted conditions. Cells were pre-treated with 50 μM BSO for 24 h and then treated or not with 20 μM MG132 for 2 h, followed by treatment with H_2O_2 for 2 h. (A) The degrees of phosphorylation of mTOR at Ser 2481 and p70S6K at Thr 389, the levels of p62 and Rheb expression were determined by western blot analysis at 2 h after H_2O_2 treatment. (B) Cell viability was assessed by an MTT assay at 2 h after H_2O_2 treatment. Similar results were observed in three independent experiments. $^*p < 0.001$ vs control cells treated with 200 μM H_2O_2.

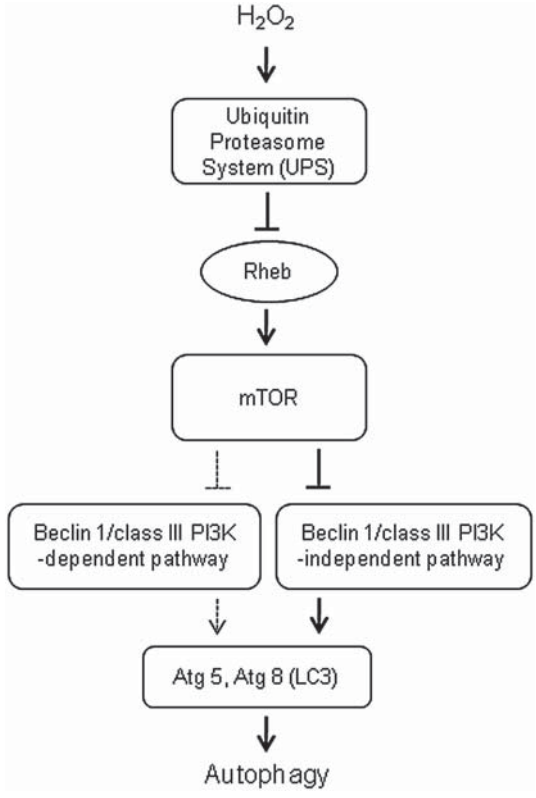

Figure 9. A schematic diagram of the signaling pathway involved in the autophagic pathway of H_2O_2-treated and GSH-depleted RAW 264.7 cells.

damage. When cells were treated with 200 μM H_2O_2, cell viability was 91% in normal conditions and was reduced up to 20% in GSH-depleted conditions (Figure 1A). These results demonstrate that intracellular GSH plays a critical role in protecting against H_2O_2 damage in RAW 264.7 cells.

In the context of GSH depletion, we compared the concentration of H_2O_2 and the duration of exposure used in our experiments with those used by Zhang et al. [7], who showed that treatment with 1000 μM H_2O_2 for 12 h reduced cell viability by 72% through autophagic cell death in malignant glioma U251 cells under non-GSH-depleted conditions. In contrast, our results showed that treatment with 50 μM H_2O_2 for 2 h, at lower concentration for a shorter time, reduced cell viability by more than 45% in RAW 264.7 cells under GSH-depleted conditions. Although the issue of whether the GSH level of U251 cells is similar to that of RAW 264.7 cells is not known, GSH-depletion by treatment with BSO renders cells more sensitive to H_2O_2-induced autophagic cell death.

BSO itself as a single agent shows cytotoxic activity, however its cytotoxicity can vary depending on the cell type being used. Even in neuroblastoma cell lines, BSO is highly cytotoxic to SMS-LHN and SMS-SAN, but not to SK-N-RA [34]. RAW 264.7 cells were also resistant to BSO cytotoxicity at 50 μM, at which the intracellular level of GSH was reduced to nearly 0% (Figure 2A). BSO (50 μM) treatment alone did not affect the cell viability of RAW 264.7 cells (Figure 2B). However, it remains uncertain whether BSO is only involved in accumulating H_2O_2 and aggravating its cytotoxic effect or contributes to H_2O_2-induced autophagic cell death in an as yet unknown fashion.

Depending on experimental conditions, H_2O_2 is capable of inducing either autophagy or autophagic cell death. Although autophagy is known to be a cytoprotective process, it has also been implicated in cell death [35]. Huang et al. [36] reported that the suppression of autophagy by the knockdown of Atg5 or Atg7 sensitized H_2O_2-induced cell death in *Bax*-/- *Bak*-/- mouse embryonic fibroblasts, suggesting that autophagy, when induced by H_2O_2, plays a cytoprotective role in H_2O_2-induced necrotic cell death. In contrast, our results showed that the down-regulation of *Atg5* by siRNA transfection protected cells from H_2O_2-induced cell death (Figure 3E), suggesting that autophagy induced by H_2O_2 functions as a type of cell death rather than as a protective mechanism in our settings.

H_2O_2 has been reported to stimulate protein catabolism by up-regulating UPS activity through various mechanisms depending on its concentration, target proteins and cell types. Li et al. [13] reported that treatment with 100 μM H_2O_2 for 6 h induced the degradation of muscle proteins by stimulating ubiquitin-conjugating activity in C_2C_{12} myotubes. In that report, the authors reported that the H_2O_2-induced ubiquitination of muscle proteins was blocked in the presence of cycloheximide, an inhibitor of protein synthesis, and actinomycin D, an inhibitor of RNA synthesis, suggesting that the process is dependent on new protein synthesis. In contrast to this report, Inukai et al. [37] reported that H_2O_2-induced ubiquitination and proteasomal degradation of Rpb1, a sub-unit of RNA polymerase II, was not inhibited in the presence of cycloheximide in HeLa cells. Consistent with the results of Inukai et al. [37], our data also indicate that the degradation of Rheb by treatment with 200 μM H_2O_2 for 2 h in the presence of BSO was not blocked by cycloheximide in RAW 264.7 cells, suggesting that the H_2O_2-induced ubiquitination and proteasomal degradation of Rheb is not dependent on new protein synthesis (Figure 7B).

In the current study, our results showed proteasome inhibition with MG132 restored the expression of Rheb and the activity of mTOR and protected cells from H_2O_2-induced autophagic cell death, demonstrating the inhibitory effect of proteasome inhibition on H_2O_2-induced autophagy (Figures 8A and B). In contrast to the results of our study, previous studies have shown that proteasome inhibitor treatment induces autophagy in various cell lines. Yang et al. [38] and Wu et al. [39] showed that treatment with MG132 induced autophagy in human prostate cancer cell line PC3 and colon adenocarcinoma cell line HT-29 cells, respectively. It has been reported that autophagy can be activated and serve as a compensatory mechanism when the UPS is suppressed [17]. In addition, treatment with MG132 has been reported to induce apoptosis in A549 cells, a lung cancer cell line [40]. Thus, the inhibitory effect of proteasome inhibition by MG132 on autophagy may be confined to a type of autophagy, which is induced by excessive proteasomal degradation of autophagy-related proteins, as shown in H_2O_2-treated and GSH-depleted RAW 264.7 cells.

H_2O_2-induced autophagy has been reported to be dependent on Beclin 1/class III PI3K [5,7]. Zhang et al. [7] showed that H_2O_2 treatment at relatively high concentration (500–1500 μM) for 12 h induced Beclin 1/class III PI3K-dependent autophagic cell death in U251 cells under non-GSH-depleted conditions. In that report, the authors indicated the importance of balance between class I and class III PI3K in the regulation of autophagy by demonstrating that H_2O_2 induced autophagy by activation of Beclin 1/class III PI3K pathway and by inhibition of class I PI3K/Akt/mTOR activity. However, this imbalance is not sufficient to explain H_2O_2-induced autophagy in our system, since our data showed that treatment with H_2O_2 did not cause an increase in Beclin 1 expression (Figure 3A) and H_2O_2-induced autophagic cell death was not blocked by the down-regulation of Beclin 1 (Figure 3C) under GSH-depleted conditions. In addition, H_2O_2-induced autophagic cell death was not inhibited by pre-treatment with PI3K inhibitors, such as 3-MA and wortmannin in GSH-depleted RAW264.7 cells (Figure 1B).

3-MA and wortmannin inhibit both class I and class III PI3K and 3-MA has been reported to promote autophagy when used under nutrient-rich conditions for more than 3 h [22], however they still have the ability to suppress starvation-induced autophagy, which is dependent on Beclin 1/class III PI3K [41]. Although it is difficult to directly compare our results with those of previous studies due to differences in experimental protocols, the reasons for these discrepancies would be helpful in terms of understanding the relationship between the Beclin 1-dependent and -independent autophagic pathways.

Autophagy, especially macroautophagy, can be classified into two categories: Beclin 1-dependent and -independent autophagy. In the case of Beclin 1-dependent autophagy, the formation of a Beclin 1/class III PI3K complex is required for the initiation of the formation of the autophagosome [30], which is followed by the conjugation of Atg12, Atg5 and LC3 to the autophagosomal membrane. This type of autophagy is classically elicited by nutrient deprivation. In the case of Beclin 1-independnet autophagy, neither Beclin 1 knockdown nor inhibitors of class III PI3K inhibit the autophagic pathway, as the name implies. While the exact regulatory mechanism of Beclin 1-independent autophagy remains unclear, there are several examples that show how Beclin 1-independent autophagy is induced. Zhu et al. [42] reported that treatment with 1-methyl-4-phenylpyridinium (MPP+), a neurotoxin, induced mitochondrial injury, resulting in Beclin 1-independent autophagic cell death in SH-SY5Y cells, a human neuroblastoma cell line. In addition, the authors showed that cell death was reversed by the inhibition of extracellular signal-regulated protein kinase (ERK) kinase, suggesting that ERK is implicated in MPP+-induced cell death. In addition, Scarlatti et al. [32] proposed an alternate mechanism for Beclin 1-independent autophagic cell death, which is different from that of MPP+-induced cell death. In that report, the authors showed that Resveratrol, a polyphenol, induced autophagic cell death, which was not inhibited by Beclin 1 and *hVPS34* siRNAs and by the inhibition of class III PI3K in MCF-7 cells, a human breast cancer cell line. The authors also showed that Resveratrol-induced cell death was associated with inhibition of Akt/protein kinase B and of mTOR signalling pathway, suggesting that Resveratrol-induced autophagy is dependent on the inhibition of mTOR. Interestingly, both MPP+ and Resveratrol-induced autophagies were characterized by increased numbers of LC3 puncta and the LC3-II/I ratio, as occurs in nutrient deprivation-induced Beclin 1-dependent autophagy. These results indicate that the mechanism of MPP+ and Resveratrol-induced Beclin 1-independent autophagy is regulated upstream of the Atg 12, Atg5 and LC3 conjugation systems.

Our results for H_2O_2 treatments at higher concentrations (100 and 200 μM) are in general agreement with results reported by Scarlatti et al. [32] in that H_2O_2 was found to suppress the Rheb/mTOR/p70S6K pathway and to induce autophagic cell death, in a Beclin 1-independent and an Atg5-dependent manner, which was also characterized by an increased LC3-II/I ratio, a decreased level of p62 and the formation of autophagic vacuoles. However, no such concentration-dependent suppression of Rheb/mTOR/p70S6K pathway was observed and only high concentrations (100 and 200 μM) of H_2O_2 caused significant inhibition of the Rheb/mTOR/p70S6K pathway (Figure 4), although autophagic cell death was observed in a range between 25–200 μM (Figure 1A). H_2O_2 treatment did not affect the phosphorylation of mTOR and p70S6K at lower concentrations (25 and 50 μM) (Figure 4), where Atg5-dependent autophagic cell death occurred (Figure 3E). These data indicate the possibility of the existence of another mechanism, which contributes H_2O_2-induced autophagic cell death at lower concentrations (25 and 50 μM) or at any concentration and thus initiates or aggravates Rheb/mTOR/p70S6K suppression at higher concentrations (100 and 200 μM). Although there may be limitation to the generalizability of our results, since Rheb/mTOR/p70S6K suppression was restricted to high concentrations of H_2O_2, our results demonstrate that the suppression of the Rheb/mTOR/p70S6K pathway by H_2O_2 functions, at least in part, as an autophagic cell death mechanism under GSH-depleted conditions.

Declaration of interest

This work was supported by the Korea Science & Engineering Foundation (KOSEF) through the MRC for Cell Death Disease Research Center at the Catholic University of Korea.

References

[1] Ott M, Gogvadze V, Orrenius S, Zhivotovsky B. Mitochondria, oxidative stress and cell death. Apoptosis 2007;12:913–922.
[2] Ng CF, Schafer FQ, Buettner GR, Rodgers VG. The rate of cellular hydrogen peroxide removal shows dependency on GSH: mathematical insight into *in vivo* H2O2 and GPx concentrations. Free Radic Res 2007;41:1201–1211.
[3] Takeda M, Shirato I, Kobayashi M, Endou H. Hydrogen peroxide induces necrosis, apoptosis, oncosis and apoptotic oncosis of mouse terminal proximal straight tubule cells. Nephron 1999;81:234–238.
[4] Jiang B, Liu JH, Bao YM, An LJ. Hydrogen peroxide-induced apoptosis in pc12 cells and the protective effect of puerarin. Cell Biol Int 2003;27:1025–1031.
[5] Chen Y, McMillan-Ward E, Kong J, Israels SJ, Gibson SB. Oxidative stress induces autophagic cell death independent of apoptosis in transformed and cancer cells. Cell Death Differ 2008;15:171–182.
[6] Scherz-Shouval R, Shvets E, Fass E, Shorer H, Gil L, Elazar Z. Reactive oxygen species are essential for autophagy and

specifically regulate the activity of Atg4. EMBO J 2007;26: 1749–1760.
[7] Zhang H, Kong X, Kang J, Su J, Li Y, Zhong J, Sun L. Oxidative stress induces parallel autophagy and mitochondria dysfunction in human glioma U251 cells. Toxicol Sci 2009; 110:376–388.
[8] Byun YJ, Kim SK, Kim YM, Chae GT, Jeong SW, Lee SB. Hydrogen peroxide induces autophagic cell death in C6 glioma cells via BNIP3-mediated suppression of the mTOR pathway. Neurosci Lett 2009;461:131–135.
[9] Zhang H, Bosch-Marce M, Shimoda LA, Tan YS, Baek JH, Wesley JB, Gonzalez FJ, Semenza GL. Mitochondrial autophagy is an HIF-1-dependent adaptive metabolic response to hypoxia. J Biol Chem 2008;283:10892–10903.
[10] Hamacher-Brady A, Brady NR, Logue SE, Sayen MR, Jinno M, Kirshenbaum LA, Gottlieb RA, Gustafsson AB. Response to myocardial ischemia/reperfusion injury involves Bnip3 and autophagy. Cell Death Differ 2007;14:146–157.
[11] Li Y, Wang Y, Kim E, Beemiller P, Wang CY, Swanson J, You M, Guan KL. Bnip3 mediates the hypoxia-induced inhibition on mammalian target of rapamycin by interacting with Rheb. J Biol Chem 2007;282:35803–35813.
[12] Yang Q, Inoki K, Kim E, Guan KL. TSC1/TSC2 and Rheb have different effects on TORC1 and TORC2 activity. Proc Natl Acad Sci USA 2006;103:6811–6816.
[13] Li YP, Chen Y, Li AS, Reid MB. Hydrogen peroxide stimulates ubiquitin-conjugating activity and expression of genes for specific E2 and E3 proteins in skeletal muscle myotubes. Am J Physiol Cell Physiol 2003;285:806–812.
[14] Ciechanover A. Proteolysis: from the lysosome to ubiquitin and the proteasome. Nat Rev Mol Cell Biol 2005;6:79–87.
[15] Lee JC, Peter ME. Regulation of apoptosis by ubiquitination. Immunol Rev 2003;193:39–47.
[16] Korolchuk VI, Menzies FM, Rubinsztein DC. Mechanisms of cross-talk between the ubiquitin-proteasome and autophagy-lysosome systems. FEBS Lett 2010;584:1393–1398.
[17] Ding WX, Ni HM, Gao W, Yoshimori T, Stolz DB, Ron D, Yin XM. Linking of autophagy to ubiquitin-proteasome system is important for the regulation of endoplasmic reticulum stress and cell viability. Am J Pathol 2007;171:513–524.
[18] Chen J, Small-Howard A, Yin A, Berry MJ. The responses of Ht22 cells to oxidative stress induced by buthionine sulfoximine (BSO). BMC Neurosci 2005;6:10.
[19] Marengo B, De Ciucis C, Verzola D, Pistoia V, Raffaghello L, Patriarca S, Balbis E, Traverso N, Cottalasso D, Pronzato MA, Marinari UM, Domenicotti C. Mechanisms of BSO (L-buthionine-S,R-sulfoximine)-induced cytotoxic effects in neuroblastoma. Free Radic Biol Med 2008;44:474–482.
[20] Iida M, Sunaga S, Hirota N, Kuribayashi N, Sakagami H, Takeda M, Matsumoto K. Effect of glutathione-modulating compounds on hydrogen-peroxide-induced cytotoxicity in human glioblastoma and glioma cell lines. J Cancer Res Clin Oncol 1997;123:619–622.
[21] Hortelano S, Garcia-Martin ML, Cerdan S, Castrillo A, Alvarez AM, Bosca L. Intracellular water motion decreases in apoptotic macrophages after caspase activation. Cell Death Differ 2001;8:1022–1028.
[22] Wu YT, Tan HL, Shui G, Bauvy C, Huang Q, Wenk MR, Ong CN, Codogno P, Shen HM. Dual role of 3-methyladenine in modulation of autophagy via different temporal patterns of inhibition on class I and III phosphoinositide 3-kinase. J Biol Chem 2010;285:10850–10861.
[23] Kiss Z, Tomono M. Wortmannin inhibits carcinogen-stimulated phosphorylation of ethanolamine and choline. FEBS Lett 1995; 358:243–246.
[24] Lee SK, Lee JS, Shin KS, Yoo SJ. Translation initiation factor 4E (eIF4E) is regulated by cell death inhibitor, Diap1. Mol Cells 2007;24:445–451.
[25] Allende CC, Hinrichs MV, Santos E, Allende JE. Oncogenic ras protein induces meiotic maturation of amphibian oocytes in the presence of protein synthesis inhibitors. FEBS Lett 1988;234:426–430.
[26] Rahman I, Kode A, Biswas SK. Assay for quantitative determination of glutathione and glutathione disulfide levels using enzymatic recycling method. Nat Protoc 2006;1:3159–3165.
[27] Rachek LI, Musiyenko SI, LeDoux SP, Wilson GL. Palmitate induced mitochondrial deoxyribonucleic acid damage and apoptosis in l6 rat skeletal muscle cells. Endocrinology 2007;148: 293–299.
[28] Yamamoto A, Tagawa Y, Yoshimori T, Moriyama Y, Masaki R, Tashiro Y. Bafilomycin A1 prevents maturation of autophagic vacuoles by inhibiting fusion between autophagosomes and lysosomes in rat hepatoma cell line, H-4-II-E cells. Cell Struct Funct 1998;23:33–42.
[29] Klionsky DJ, Abeliovich H, Agostinis P, Agrawal DK, Aliev G, Askew DS, et al. Guidelines for the use and interpretation of assays for monitoring autophagy in higher eukaryotes. Autophagy 2008;4:151–175.
[30] Furuya N, Yu J, Byfield M, Pattingre S, Levine B. The evolutionarily conserved domain of Beclin 1 is required for Vps34 binding, autophagy and tumor suppressor function. Autophagy 2005;1:46–52.
[31] Codogno P, Meijer AJ. Atg5: more than an autophagy factor. Nat Cell Biol 2006;8:1045–1047.
[32] Scarlatti F, Maffei R, Beau I, Codogno P, Ghidoni R. Role of non-canonical Beclin 1-independent autophagy in cell death induced by resveratrol in human breast cancer cells. Cell Death Differ 2008;15:1318–1329.
[33] Zhou X, Ikenoue T, Chen X, Li L, Inoki K, Guan KL. Rheb controls misfolded protein metabolism by inhibiting aggresome formation and autophagy. Proc Natl Acad Sci USA 2009;106:8923–8928.
[34] Anderson CP, Tsai JM, Meek WE, Liu RM, Tang Y, Forman HJ, Reynolds CP. Depletion of glutathione by buthionine sulfoxine is cytotoxic for human neuroblastoma cell lines via apoptosis. Exp Cell Res 1999;246:183–192.
[35] Berry DL, Baehrecke EH. Growth arrest and autophagy are required for salivary gland cell degradation in Drosophila. Cell 2007;131:1137–1148.
[36] Huang Q, Wu YT, Tan HL, Ong CN, Shen HM. A novel function of poly(ADP-ribose) polymerase-1 in modulation of autophagy and necrosis under oxidative stress. Cell Death Differ 2009;16:264–277.
[37] Inukai N, Yamaguchi Y, Kuraoka I, Yamada T, Kamijo S, Kato J, Tanaka K, Handa H. A novel hydrogen peroxide-induced phosphorylation and ubiquitination pathway leading to RNA polymerase II proteolysis. J Biol Chem 2004;279: 8190–8195.
[38] Yang W, Monroe J, Zhang Y, George D, Bremer E, Li H. Proteasome inhibition induces both pro- and anti-cell death pathways in prostate cancer cells. Cancer Lett 2006;243:217–227.
[39] Wu WK, Wu YC, Yu L, Li ZJ, Sung JJ, Cho CH. Induction of autophagy by proteasome inhibitor is associated with proliferative arrest in colon cancer cells. Biochem Biophys Res Commun 2008;374:258–263.
[40] Han YH, Park WH. MG132 as a proteasome inhibitor induces cell growth inhibition and cell death in A549 lung cancer cells via influencing reactive oxygen species and GSH level. Hum Exp Toxicol 2010;29:607–614.
[41] Munafo DB, Colombo MI. A novel assay to study autophagy: regulation of autophagosome vacuole size by amino acid deprivation. J Cell Sci 2001;114:3619–3629.
[42] Zhu JH, Horbinski C, Guo F, Watkins S, Uchiyama Y, Chu CT. Regulation of autophagy by extracellular signal-regulated protein kinases during 1-methyl-4-phenylpyridinium-induced cell death. Am J Pathol 2007;170:75–86.

This paper was first published online on Early Online on 11 November 2010.